

# Implementation of a Modified Anisotropic Creep Model with structure for soft soils with the Use of COMSOL Physics Builder

M. Karlsson\*<sup>1</sup> and J. Yannie<sup>1</sup>

<sup>1</sup>Division of GeoEngineering, Chalmers University of Technology, <sup>1</sup>

\*Corresponding author: Sven Hultins gata 8, SE-412 96, Gothenburg, Sweden, mats.karlsson@chalmers.se

**Abstract:** In this paper an anisotropic creep model including structure is implemented in COMSOL v.5.2 and is validated against different laboratory tests such as Constant Rate of Strain (CRS) and K<sub>0</sub>-consolidated undrained triaxial tests in both compression and extension. The implementation in COMSOL is conducted by using a fully coupled analysis between the Solid Mechanics node and the Darcy law node together with the user defined constitutive model created in the Physics Builder. In the Solid Mechanics the user defined model is called from the creep sub node and in this case the potential model is used where the rate multiplier and the creep (plastic) potential is given. The physics builder has been used to define the main body of the constitutive model such as the rotation law that determines the anisotropic behaviour of the model, the structure in the soil and both the rate multiplier and creep potential surface. The physics builder enables the user a possibility to create a constitutive model with a huge number of complex equation together with a graphical user interface. The implemented constitutive model is able to capture both the rate dependency, the anisotropy and the structure observed in soft soils such as clays.

**Keywords:** Soft soil, creep, numerical implementation.

## 1. Introduction

Soil improvement and construction of building foundations or embankments can be quite complicated and expensive in such areas. Therefore, construction costs need to be balanced against high maintenance costs. In order to do this optimally, there is a need to predict long-term settlement with a higher degree of accuracy. To be able to predict long-term settlements of buildings and infrastructure foundations on soft soils it is necessary to include the effect of creep.

In this paper a Modified Anisotropic Creep model with structure (herein called MAC-s) is implemented in COMSOL. The constitutive

model is validated against a number of different laboratory tests, such as Constant Rate of Strain oedometer tests (CRS) and K<sub>0</sub>-Consolidated Undrained triaxial tests (K<sub>0</sub>CU) in both compression and extension stress paths.

## 2. The Modified Anisotropic Creep model with structure

The material model implemented in COMSOL is based on the SCLAY1S model and the n-SAC model developed by Karstunen et al. (2005) and Grimstad & Degago (2010), respectively. The difference between the MAC-s model and the CREEP-SCLAY1S model is that the former has a different intrinsic and normal compression surface (NCS), but uses the SCLAY1S surface as the plastic potential. Therefore, the model is of the non-associative type. This creep model is based on the extension from the one-dimensional formulation to a general three-dimensional constitutive model by Vermeer et al. (1998).

### 2.1 Elastic behaviour

The MAC-s model makes use of the same type of stress dependent formulation for the elastic parameters as the Modified Cam-Clay type of models i.e. the tangent bulk modulus is defined according to eq. (1).

$$K' = \frac{p'}{\kappa^*} \quad (1)$$

where  $\kappa^*$  is the slope of swelling line and  $p'$  is mean effective stress. The shear modulus,  $G$ , is calculated based on the bulk modulus with the assumption of a constant Poisson's ratio,  $\nu'$ , see eq. (2).

$$G = \frac{3(1-2\nu')}{2(1+\nu')} \cdot K' \quad (2)$$

## 2.2 Normal compression and plastic potential surface

The normal compression surface  $F$  of the MAC-s model is defined in general stress space according to eq. (3).

$$F = \frac{1}{2}(\mathbf{s})^T (\mathbf{s}) - p'^2 \cdot \left(1 - \left(\frac{p'}{p_c}\right)^m\right) \cdot \left(M^2 - \frac{1}{2}\mathbf{a}_d^T \mathbf{a}_d\right) \quad (3)$$

where  $\mathbf{s} = \boldsymbol{\sigma}_d - p' \cdot \mathbf{a}_d$  and the exponent  $m$  in eq. (3) controls the shape, slenderness, of the normal consolidation surface. Using the equivalent mean stress,  $p_{eq}$ , the normal consolidation surface is formulated according to eq. (4).

$$p_{eq} = \frac{p'}{\left[1 - \frac{\frac{1}{2}\{\boldsymbol{\sigma}_d - p' \cdot \mathbf{a}_d\}^T \{\boldsymbol{\sigma}_d - p' \cdot \mathbf{a}_d\}}{p'^2 \cdot \left(M^2 - \frac{1}{2}\{\mathbf{a}_d\}^T \{\mathbf{a}_d\}\right)}\right]^{\frac{1}{m}}} \quad (4)$$

The plastic potential that is used for this model has the same shape as the CREEP-SCLAY1S model, i.e. the rotated ellipsoid according to eq. (5).

$$p_Q^{eq} = p' + \frac{3}{2} \cdot \frac{\{\boldsymbol{\sigma}_d - p' \cdot \mathbf{a}_d\}^T \{\boldsymbol{\sigma}_d - p' \cdot \mathbf{a}_d\}}{p' \cdot \left(M^2 - \frac{3}{2}\{\mathbf{a}_d\}^T \{\mathbf{a}_d\}\right)} \quad (5)$$

A visualization of the new normal compression surface, NCS, and the plastic potential surface in  $p'$ - $q$  stress space is shown in Figure 1. The influence of different  $m$  values are displayed in Figure 2. The MAC-s model makes use of the visco-plastic multiplier see eq. (6).

$$\dot{\lambda} = \frac{1}{r_{si} \cdot \tau} \cdot \left(\frac{p^{eq}}{(1 + \chi) \cdot p'_{ci}}\right)^{r_{si}(\lambda_i^* - \kappa^*)} \cdot \frac{M_c^2 - \alpha_0^2}{M_c^2 - \eta_0^2} \quad (6)$$

where  $M_c$  is critical state line in compression and  $\alpha_0$ , is the rotation of the potential surface in  $K_0^{NC}$  loading and  $\eta_0$  is the stress path corresponding to  $K_0^{NC}$  loading. The MAC-s model also incorporates structure or bonding, as described for the S-CLAY1S model, based on the formulation by Gens & Nova (1993).

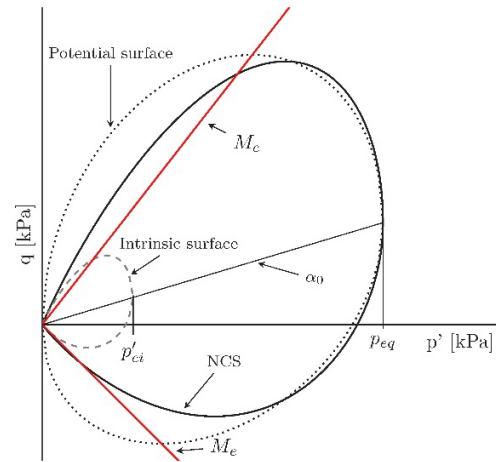


**Figure 1.** Visualisation of the NCS (solid line) of the MAC-s model with  $m=0.4$  compared with plastic potential surface (dotted line) in  $p'$ - $q$  stress space together with the intrinsic surface, the failure criteria and the  $\alpha_0$ -line.

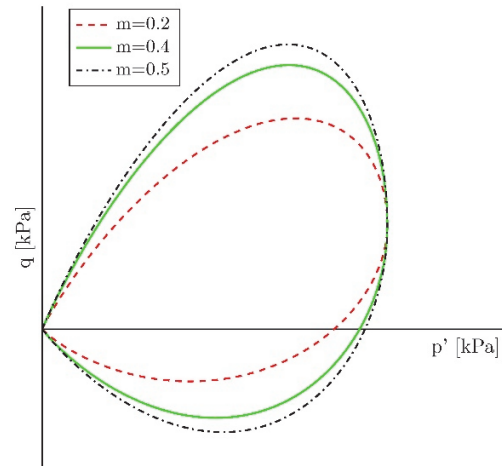


**Figure 2.** Visualisation of the effect of different  $m$ -values are shown in  $p'$ - $q$  stress space.

## 2.3 Hardenings laws

The MAC-s model incorporates three different hardening laws. The hardening laws are the same as for the CREEP-SCLAY1S model. The first hardening law is controlling the change in the size of the intrinsic reference surface with respect to the volumetric creep strains ( $\varepsilon_v^c$ ),

similar to that of Modified Cam-Clay, according to eq. (7).

$$p_{ci} = p_{ci0} \exp\left(\frac{\varepsilon_v^c}{\lambda_i^* - \kappa^*}\right) \quad (7)$$

where  $\lambda_i^*$  and  $\kappa^*$  are the modified compression index and modified swelling index respectively, evaluated from a “ $\ln p' - \varepsilon_v$ ” plot. The parameter  $p_{ci0}$  is the initial preconsolidation pressure at the hydrostatic axis and the subscript “i” means the intrinsic parameter.

The second hardening law is describing the rotation of the reference surface, i.e. the evolution of the anisotropy, due to creep strains similarly to eq. (8).

$$d\mathbf{a}_d = \left( \omega_v \left[ \frac{3\boldsymbol{\eta}}{4} - \mathbf{a}_d \right] \cdot \langle d\varepsilon_v^c \rangle + \omega_d^* \left[ \frac{\boldsymbol{\eta}}{3} - \mathbf{a}_d \right] \cdot d\varepsilon_d^c \right) \quad (8)$$

where  $\boldsymbol{\eta}$  the generalised stress ratio, defined as  $\boldsymbol{\eta} = \boldsymbol{\sigma}_d / p'$ , and  $\varepsilon_d^c$  is the deviatoric creep strain.

The third hardening law describes the degradation of bonding in the soil and is defined by an intrinsic reference surface. The intrinsic reference surface has the same shape and inclination, but differs in size with respect to the normal compression surface i.e. the normal compression surface of the bonded soil. The size of the intrinsic reference surface is related to the normal compression surface by a parameter  $\chi$  which determines the current degree of bonding according to eq. (9).

$$p_c = (1 + \chi) \cdot p_{ci} \quad (9)$$

where  $p_{ci}$  is the intrinsic preconsolidation pressure at the hydrostatic axis. The degradation of bonding is associated with volumetric and deviatoric creep strains and formulated according to eq. (10).

$$d\chi = -\chi \left( \xi_v |d\varepsilon_v^c| + \xi_d |d\varepsilon_d^c| \right) \quad (10)$$

where  $\xi_v$  and  $\xi_d$  are additional soil constants controlling the rate of degradation.

### 3. Implementation in Physics Builder

The Physics Builder in COMSOL has been used for several reasons as the major tool for implementing the MAC-s model. Some of the important ones are:

- User friendly interface for adding complexity to a model step-by-step manner.
- Possible to create a user defined physics interface for easy sharing.
- Simple to create a GUI that shows the implemented equations and parameters.
- Easy to create complex equation in a simple and effective manner.

The implementation of the model is so that the solid mechanics node communicates with the user defined physics node (MAC-s model) and the Darcy law node (excess pore pressure), see Figure 3.

The user defined physics node containing the MAC-s model interacts with the creep subnode under the linear elastic material model in the solid mechanics node. The potential creep model is used and the rate multiplier and creep potential is interacting with the user defined model by calling the respective variable name from the MAC-s model.

The stresses and the creep strains from the solid mechanics node are passed to the MAC-s model and updates all parameters, continuously. The Darcy law node is used to calculate the excess pore pressure that relates from the volumetric strain. This is then passed back to the linear elastic model by an external stress subnode. All three physics nodes are fully coupled during the calculation to ensure the most accurate stress and strains.

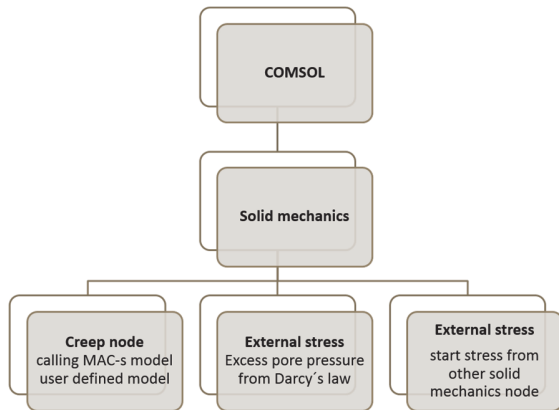


Figure 3. Hierarchy for the model.

#### 4. Validation of the model

In order to see how well the MAC-s model, represents real soil behaviour, a number of simulations are conducted as boundary value problems modelled with COMSOL. The common input parameters for all the simulations are summarized in Table 1. The vertical preconsolidation pressure, used in the simulations was set to 100 kPa for the triaxial and Constant Rate of Strain (CRS) tests at 10 m depth. The vertical preconsolidation pressure was set to 350 kPa in the simulation of the triaxial test of 45 m depth. The input values of  $K_0^{nc}$ ,  $\alpha_0$  and  $\omega_d$  is calculated as described in Olsson (2013). The un-/reload Poisson's ratio was set to 0.2 and the factor m controlling the shape of the NCS is set to 0.4. The reference time,  $\tau$ , is set to 1 day.

Table 1. Input parameters for simulations.

$\phi'$	$\kappa^*$	$\lambda_i^*$	$r_{si}$	$\omega_v$	$\omega_d^*$
32°	0.016	0.075	700	200	170

$\chi_0$	$\xi_v$	$\xi_d$	$M_e$	$M_c$	$\alpha_0$
20	13	5	1	1.287	0.491

The results of the simulations are presented in Figure 4 to Figure 6 and are compared with the corresponding laboratory result. In Figure 4 a CRS oedometer test is simulated and compared

with laboratory results for a clay sample from 10 m depth. The simulated stress–strain curve has a relatively good agreement with the laboratory results, except around the preconsolidation pressure, where the simulation predicts a much more sudden transition than the laboratory curve.

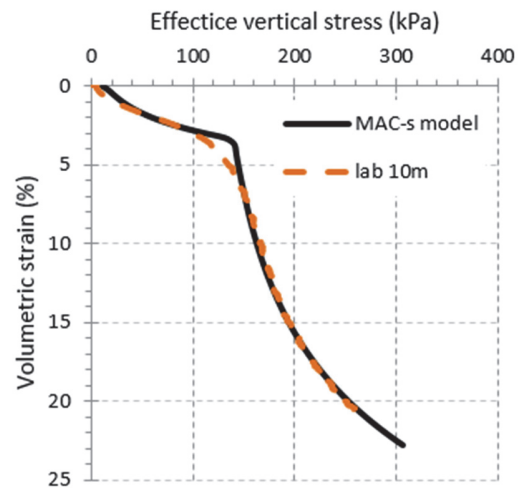
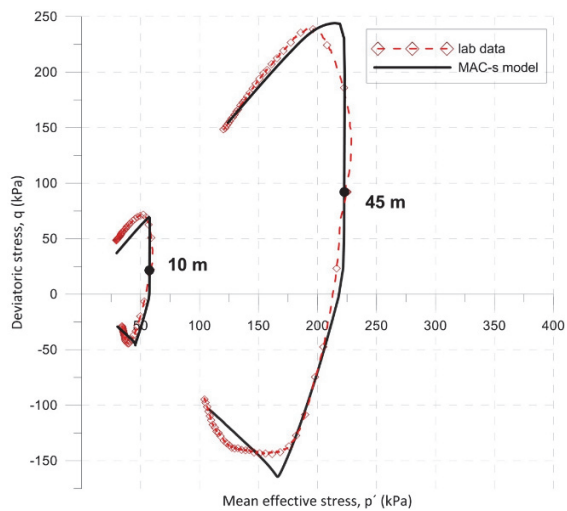


Figure 4. Stress-strain curve of simulation result compared with laboratory result of a CRS oedometer test at the depth of 10 m.

In Figure 5 and Figure 6 four  $K_0$ -consolidated undrained triaxial tests are simulated and compared with the corresponding laboratory test, in  $p'$ - $q$  stress space plot and  $q$ -axial strain plot, respectively. As shown in Figure 5 the MAC-s model is in good agreement with experimental results in  $p'$ - $q$  stress space. However, it seems that the compression test of 10 m depth is slightly under predicted.

For the extension tests the simulated stress paths are in good agreement with experimental results, i.e. following the stress path until a certain stress level where the experimental results decrease faster in mean effective stress than predicted by the model. Based on Figure 6 the predicted deviatoric stress versus axial strain is in good agreement with the experimental data. However, the sample from the depth of 45 m seems to behave in stiffer manner in the simulation compared with the experimental data when approaching the peak strength.



**Figure 5.** Simulations results (solid black lines) compared with laboratory results (dashed red lines with squares). Black dots indicate the  $K_0$ -consolidated stress state just before the undrained shearing.

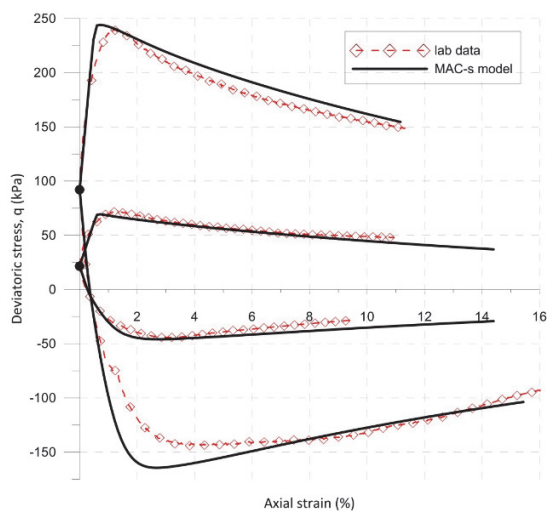


**Figure 6.** Simulation results (solid black lines) compared with laboratory results (dashed red lines with squares). Black dots indicate the  $K_0$ -consolidated stress state just before the undrained shearing.

## 6. Conclusions

This paper describes the implementation of an anisotropic creep model including structure (MAC-s) in COMSOL.

The validation of MAC-s model by comparison with laboratory tests show very good agreement with both laboratory tests shown in this paper. The model seems to capture both the compression and the extension side of  $K_0$ -consolidated triaxial tests at different stress levels. However, the stiffness seems to be overestimated in the simulation for the 45 m depth tests when approaching the peak value.

Using COMSOL and the Physics Builder gives great advantages as it offers a user friendly interface for adding complexity to a model step-by-step manner without the need of any in-depth skills in programming. Most importantly, one could easily share the Physic Builder model to be used for any appropriate problem.

## 7. References

- Gens, A., & Nova, R. (1993). *Conceptual bases for a constitutive model for bonded soils and weak rocks*. Paper presented at the Proc. of Int. Symp. on Hard soils - Soft Rocks, Athens.
- Grimstad, G., & Degago, G. (2010). A non-associated creep model for structured anisotropic clay (n-SAC) *Numerical Methods in Geotechnical Engineering (NUMGE 2010)* (pp. 3-8): CRC Press.
- Karstunen, M., Krenn, H., Wheeler, S. J., Koskinen, M., & Zentar, R. (2005). Effect of Anisotropy and Destructuration on the Behaviour of Murro Test Embankment. *International Journal of Geomechanics*, *5*(2), 87-97.
- Olsson, M. (2013). *On Rate-Dependency of Gothenburg Clay*. (Phd thesis), Chalmers tekniska högskola.
- Vermeer, P. A., Stolle, D. F. E., & Bonnier, P. G. (1998). *From the classical theory of secondary compression to modern creep analysis*. Paper presented at the Proc. Computer Methods and advances in Geomechanics, Wuhan, China.